Data-driven modeling and monitoring of fuel cell performance

Ke Sun [a,*], *Iñaki Esnaola* [a,b], *Okechukwu Okorie* [c], *Fiona Charnley* [c], *Mariale Moreno* [c], *Ashutosh Tiwari* [a]

[a] *Department of Automatic Control and Systems Engineering, University of Sheffield, Sheffield S1 3JD, UK*
[b] *Department of Electrical Engineering, Princeton University, Princeton NJ 08540, USA*
[c] *Exeter Centre for Circular Economy, Exeter Business School, University of Exeter, Exeter EX4 4PU, UK*

HIGHLIGHTS

- Data-driven modeling framework for fuel cell voltage-current performance curve.
- Performance forecasting based on Gaussian process learning techniques.
- Optimal sensing of performance curve based on information-theoretic techniques.

GRAPHICAL ABSTRACT
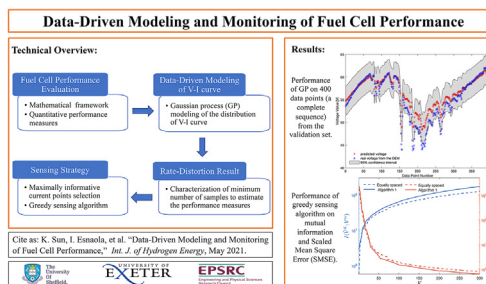
ARTICLE INFO

ABSTRACT

A mathematical framework that provides practical guidelines for user adoption is proposed for fuel cell performance evaluation. By leveraging the mathematical framework, two measures that describe the average and worst-case performance are presented. To facilitate the computation of the performance measures in a practical setting, we model the distribution of the voltages at different current points as a Gaussian process. Then the minimum number of samples needed to estimate the performance measures is obtained using information-theoretic notions. Furthermore, we introduce a sensing algorithm that finds the current points that are maximally informative about the voltage. Observing the voltages at the points identified by the proposed algorithm enables the user to estimate the voltages at the unobserved points. The proposed performance measures and the corresponding results are validated on a fuel cell dataset provided by an industrial user whose conclusion coincides with the judgement from the fuel cell manufacturer.

---

* Corresponding author.
E-mail addresses: ke.sun@sheffield.ac.uk, cn.kesun@gmail.com (K. Sun), esnaola@sheffield.ac.uk (I. Esnaola), o.s.okorie@exeter.ac.uk (O. Okorie), f.charnley@exeter.ac.uk (F. Charnley), mariale8@gmail.com (M. Moreno), a.tiwari@sheffield.ac.uk (A. Tiwari).

Introduction

Hydrogen is a clean energy source whose combustion only releases water. As a result, hydrogen energy is an effective way to reduce carbon emission and achieve a low-carbon economy [1] or carbon-neutral [2]. Furthermore, hydrogen is one of the most promising energy carriers for the future [3], 1 kg of hydrogen contains 33.33 kWh of useable energy, whereas petrol and diesel only hold about 12 kWh [4]. The fuel cell is the commonly adopted medium to convert the chemical energy of hydrogen into electricity and is used in different applications, such as vehicles and stationary power generation. However, the limited durability and reliability of fuel cells are the main barriers that halt the commercialization of this clean energy alternative [5]. To overcome these barriers, fuel cell state monitoring techniques that enable practical durability and reliability assessment are essential. Aided by these techniques, the user monitors the state of the fuel cell in a real-time manner, which is usually done by sensing the parameters that indicate the state of the fuel cell at a given frequency. In this way, the user extracts useful information about the state of the fuel cell via visualization and data-driven techniques. This information enables the user to evaluate the durability and reliability of fuel cells.

The assessment of fuel cell performance is the first and the most important step to evaluating the durability and reliability of fuel cells. There are various ways for the assessment but mostly rely on the voltage-current (V–I) curve of the fuel cell [6,7]. The V–I curve is usually obtained by experimental approaches [8,9], physical modeling approaches [10,11], and data-driven approaches [12,13]. The experimental approaches obtain the voltage at different current points by changing the operation conditions, such as changing the loads [7], to get the curve. These approaches provide the V–I curve directly but also induce high testing costs. The physical modeling approaches model the electrochemical properties of the fuel cell, such as using the Nernst equation [10] or other equations in [14], and get the parameters from the physical world. While the physical models provide a better physical understanding about the fuel cell, they are usually simplified models of the underlying complex processes in order to ease the model derivation, and therefore, their characterization capabilities are limited. Unlike the two approaches mentioned above, the data-driven approaches learn the curve from the operating data of the fuel cell using different learning algorithms, such as support vector machines [12] and neural networks [13]. The data-driven approaches enable the estimation and prediction of the unmeasured operating points, which require a large amount of operating data to obtain an accurate result [15]. More recently, learning algorithms, such as deep learning algorithms [16], have been proposed but these approaches incur on high computational complexity.

Data-driven techniques leap over the modeling challenges posed by complex systems by estimating the main features of the system from data generated by the system. In addition to V–I curve modeling tasks, data-driven approaches are also widely used in different domains of the hydrogen industry, including hydrogen generation [17,18], hydrogen storage [19–23], and hydrogen utilization [24–26]. The large amount of data required by data-driven approaches makes fuel cells an ideal application to adopt these approaches, as the fuel cell state monitoring procedures generate large amounts of data during operation. Data-driven tools are utilized in [27–29] to control the oxygen excess ratio and maximize the power generation of the fuel cell and in [30–32] to detect abnormal operating conditions. Furthermore, in [33–37], data-driven approaches are used to predict the performance degradation of the fuel cell, which is mainly described by the degradation in the V–I curve. The data-driven approaches utilized for performance evaluation include neural networks [33,35–37], principle component analysis [34], support vector machine [38], and other standard statistical learning techniques. In particular, [35] proposes a sensitivity-based algorithm that selects sensors based on the fluctuations of the parameters that describe the state of the fuel cell. However, some of the parameters chosen by the algorithm in [35] are not easy to sense and require a lab environment. Also the approaches in [35–37] define the performance of the fuel cell in a visual and qualitative manner, without mathematical expressions that provide a quantitative performance evaluation.

In this paper, we propose a mathematical framework for the evaluation of fuel cell performance from the user side, and use machine learning and information-theoretic tools to facilitate the modeling and estimation of the proposed performance measure. Specifically, we present a mathematical framework that enables a practical performance evaluation by the users and devise measures for average and worst-case performance based on the proposed framework. Since the performance measures are usually estimated from fuel cell operation data, the amount of data governs the accuracy of the estimation. To find the minimum number of samples needed to get an accurate estimate of the performance, we model the distribution of the voltages of the fuel cell at different operating current points as a Gaussian process (GP) and use rate-distortion theory results to characterize the minimum number of samples needed. Furthermore, we propose a sensing strategy to choose the operating current points that contain more information about the vector of the voltages by introducing a novel greedy algorithm that outperforms conventional uniform sensing. By observing the voltages at the current points chosen by the algorithm, the user can estimate the voltages of the unobserved points and estimate the proposed performance measure.

The main contributions of the paper are listed in the following.

- We propose a general mathematical framework for quantitatively characterizing the estimation of fuel cell V–I curves.
- We provide a model for fuel cells based on GP that adaptively incorporates data that refine the characterization in a flexible manner.
- We propose a novel fuel cell state monitoring technique that leverages information-theoretic tools for the first time in this application domain. The proposed sensing algorithm identifies the sensing points that maximize the information acquisition using only second order statistics.

Mathematical modeling of fuel cell performance

Voltage-current curve for a fuel cell

The efficiency or performance of a fuel cell is usually measured by the polarization curve, which shows the change of the potential of the fuel cell when the current density (load) changes [39–41]. An illustrative example of the polarization curve is shown in Fig. 1a, in which the performance or efficiency of the fuel cell 2 is higher than that of the fuel cell 1 as more power is generated by the fuel cell 2 per unit area.

A commercial fuel cell provided by the manufacturer to the users consists usually of several individual fuel cells that the manufacturer stacks to achieve higher voltage and power. Since commercial fuel cells are typically manufactured with a fixed area design that is not configurable by the user, we study the performance of the V–I curve instead of the polarization curve. The distinction is illustrated in Fig. 1b, where the horizontal axis is changed from current density to current and the vertical axis is changed from potential to stack voltage.

Furthermore, the fuel cell manufacturer provides the users with a *typical V–I curve*, which shows the performance of the fuel cell during the initial factory acceptance testing. The user compares the performance of the fuel cell with the typical V–I curve to assess the state of the fuel cell product.

The original equipment manufacturer (OEM) is a user that utilizes fuel cells as the energy source for its electric vehicles. Fig. 2a and Fig. 2b show the electric vehicle that is designed and manufactured by the OEM and the fuel cell adopted for the electric vehicle, respectively, in which the location of the fuel cell is marked by a red frame. The performance assessment procedure adopted by the OEM is described in the following. For a given operating current:

● If the corresponding voltage is smaller than the voltage value obtained from the typical V–I curve, then the performance of the fuel cell is suboptimal. The lower the corresponding voltage is, the worse the performance of the fuel cell is.

● If the corresponding voltage is larger than the voltage value obtained from the typical V–I curve, then the performance of the fuel cell is optimal. The fuel cell is assumed to exhibit an ideal response as long as the corresponding voltage is larger than the typical value.

In the following, we propose a quantitative framework for the practical performance measure adopted by the OEM.

Pointwise and functional performance measure

Given an operating current of the fuel cell, the corresponding voltage of the fuel cell is given by

$$V = f(i) + Z, \tag{1}$$

where $i \in \mathbb{R}_+$ is a given current point, $V \in \mathbb{R}_+$ is the corresponding voltage at this point, Z is the system noise induced by the sensor and assumed following a Gaussian distribution $\mathcal{N}(0, \sigma^2)$ with σ^2 denoting the variance of the noise, and $f : \mathbb{R}_+ \to \mathbb{R}_+$ is the mapping between the current and the noiseless voltage with $\mathbb{R}_+$ denoting the set of all positive real numbers. Similarly, the ideal voltage of the fuel cell for a given operating current is defined as

$$v^\star = f^\star(i), \tag{2}$$

where $v^\star \in \mathbb{R}_+$ is the ideal voltage of the fuel cell and $f^\star : \mathbb{R}_+ \to \mathbb{R}_+$ is the ideal mapping between the current and the voltage. Here $f^\star$ represents the relation between the current and the voltage determined by the typical V–I curve, which characterizes the ideal performance of the fuel cell.

The definition of quantitative performance measures is arbitrary in nature, as it depends on the importance that is given to the different features describing the functioning of the fuel cell. In the following, we state properties that are desirable for a practical performance measure and proceed to propose a quantitative measure that allows for an appraising of the features. We start with the pointwise definition of performance. Let $\eta : \mathbb{R}_+ \to [0, L]$ be the pointwise performance measure with $L \in \mathbb{R}_+$ denoting the maximum of the measure and v takes values in $\mathbb{R}_+$, the performance measure should
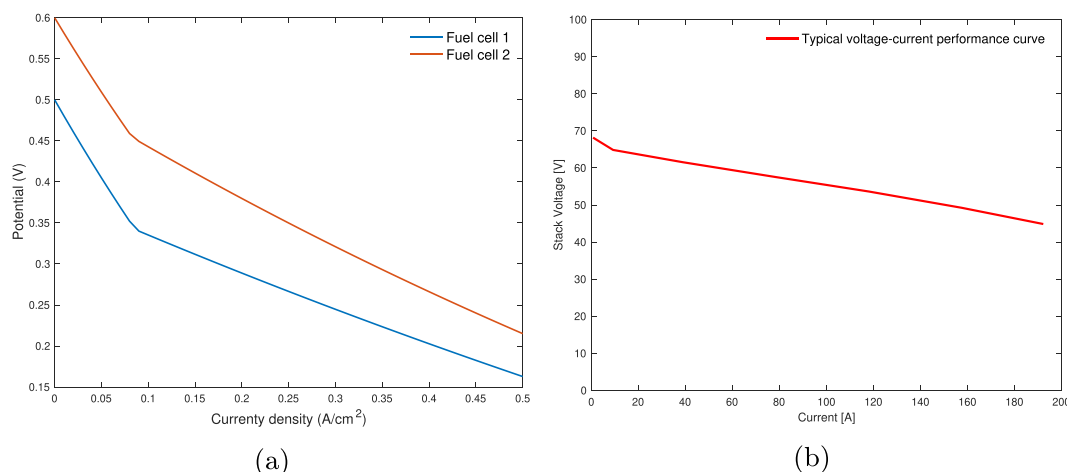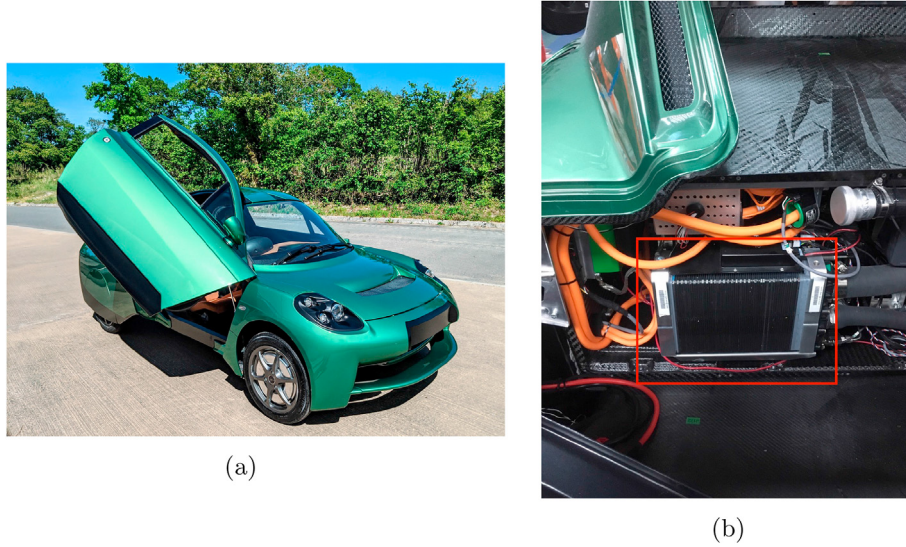

(a)

(b)

Fig. 1 – An illustrative example of: (a) the polarization curve and (b) the typical voltage-current curve.

(a)

(b)

Fig. 2 – Electric vehicle designed and manufactured by the OEM. (a) the electric vehicle (b) the fuel cell.

satisfy the following three properties when we take into account the practical performance evaluation discussion in the previous section. Let $v, v' \in \mathbb{R}_+$,

- If $v \leq v^\star$, then $\eta(v) \leq L$,
- If $v > v^\star$, then $\eta(v) = L$,
- If $v \leq v' < v^\star$, then $\eta(v) \leq \eta(v') \leq L$,

which guarantees that

- A voltage that is lower than the ideal value yields a degraded performance measure, i.e. $\eta \leq L$,
- A voltage that is higher than the ideal value yields a full performance measure, i.e. $\eta = L$,
- For any two voltages that are lower than the ideal voltage, the higher one yields a higher performance measure, i.e. $\eta(v) \leq \eta(v') \leq L$,

respectively. The value of L is tuned according to the practical requirements of the user. A high value of L implies that η takes values over a larger interval and yields more precision.

Thus, we propose the pointwise performance measure given by

$$\eta(v) = L\left(1 - \frac{1}{(v^\star)^2}(\max\{v^\star - v, 0\})^2\right) \tag{3}$$

that satisfies the requirements given above, where $\max\{a, b\}$ denotes the maximum between a and b, or the elementwise maximum for multidimensional case. The functional performance measure is obtained by extending the pointwise performance measure to the multidimensional case, which yields

$$\eta_m(\boldsymbol{v}) = L\left(1 - \frac{1}{\|\boldsymbol{v}^\star\|_2^2}\|\max\{\boldsymbol{v}^\star - \boldsymbol{v}, \boldsymbol{0}\}\|_2^2\right), \tag{4}$$

where $\eta_m : \mathbb{R}_+^m \to [0, L]$ is the functional performance measure, $\boldsymbol{v} = [v(i_1), ..., v(i_m)]^T$ is the vector of voltages at current point i_j, $j \in \{1, ..., m\}$, $\boldsymbol{v}^\star = [v^\star(i_1), ..., v^\star(i_m)]^T$ is the vector of ideal

voltages at the same current points, and $\boldsymbol{0}$ is a vector of proper dimension for which all entries are zero.

It is worth mentioning that the performance measures in (3) and (4) are not unique and can be defined in different ways. The definition can be generalized by extending it to the ℓ_p norm. For example, changing the ℓ_2 norm into the ℓ_1 norm guarantees that large deviations of voltage from the ideal voltage are not penalized.

Average and worst-case performance measure

The performance measure for fuel cell efficiency can also be defined using the pointwise performance measure in (3) for the average scenario and for the worst-case scenario. The average performance describes the overall performance of the fuel cell for different values of the current. Assume that the current $i \in \mathcal{I}$ is uniformly distributed over the discrete alphabet $\mathcal{I}$, then the average performance is given by

$$\Gamma(\eta) = \frac{1}{|\mathcal{I}|} \sum_{i \in \mathcal{I}} \eta(v(i)), \tag{5}$$

where $|\mathcal{I}|$ is the cardinality of $\mathcal{I}$. Specifically for the pointwise performance measure in (3), the average performance is given by

$$\Gamma(\eta) = \frac{1}{|\mathcal{I}|} \sum_{j=1}^{|\mathcal{I}|} L\left(1 - \frac{1}{(v^\star(i_j))^2}(\max\{v^\star(i_j) - v(i_j), 0\})^2\right). \tag{6}$$

Similarly, the worst-case performance measure is defined as

$$\underline{\eta} = \min_{i \in \mathcal{I}} \eta. \tag{7}$$

Specifically for the pointwise performance measure in (3), the worst-case performance for the discrete case is given by

$$\underline{\eta} = \min_{i \in \mathcal{I}} L\left(1 - \frac{1}{(v^\star(i))^2}(\max\{v^\star(i) - v(i), 0\})^2\right). \tag{8}$$

Generalization of performance measure

The pointwise performance measure η in (3) and the functional performance measure η_m in (4) are normalized by $(v^\star)^2$ and $\|v^\star\|_2^2$, respectively. This guarantees that the performance measures η and η_m are confined to the interval between zero and L. This implies that we assume the voltage value of zero as the minimum useable voltage for the fuel cell. In practical settings, the fuel cell may be considered as nonusable when the voltage is smaller than a certain percent of the ideal value. For example, Fig. 3 identifies the useable range for a fuel cell that generates at least 70% of the ideal voltage. This case is handled by changing the denominator and the nominator of η and η_m as

$$\eta_g = L\left(1 - \frac{1}{((1-\alpha)v^\star)^2}(\text{med}\{v^\star - v, (1-\alpha)v^\star, 0\})^2\right) \quad (9)$$

and

$$(\eta_m)_g = L\left(1 - \frac{1}{\|(1-\alpha)v^\star\|_2^2}\|\text{med}\{v^\star - v, (1-\alpha)v^\star, 0\}\|_2^2\right), \quad (10)$$

where $\eta_g : \mathbb{R}_+ \to [0, L]$ is the generalized pointwise performance measure, $(\eta_m)_g : \mathbb{R}_+^m \to [0, L]$ is the generalized functional performance measure, $\alpha \in [0, 1]$ is the useable percentage set by the fuel cell user, and med$\{a, b, c\}$ denotes the median among a, b, and c, or elementwise median for multidimensional case. The generalized performance measure in (9) and (10) can be further generalized by replacing the useable range with any minimum useable voltage curve to conform with different requirements of the user.

Information-theoretic analysis for performance measure

To calculate the performance measure or the generalized performance measure, the distribution of the vector of voltages or its estimate based on sample realizations are needed. However, a perfect estimate of the performance measure requires infinitely many samples from the distribution [42, pp. 301]. In this section, we model the distribution of the vector of voltages using a GP, and provide the minimum number of voltage samples needed to obtain an estimate of the performance measure with an arbitrary accuracy. At the end of this section, we propose a greedy algorithm to select the current points that maximize the amount of information about the voltage. By observing the voltages at the chosen current points, the user is able to get a better estimate of the voltage at the other current points than with equal spaced observations.

In the following, we introduce the modeling approach for the vector of voltages using a GP.

Gaussian process

A GP is a collection of random variables for which any finite subset of variables have a joint Gaussian distribution [43]. A GP
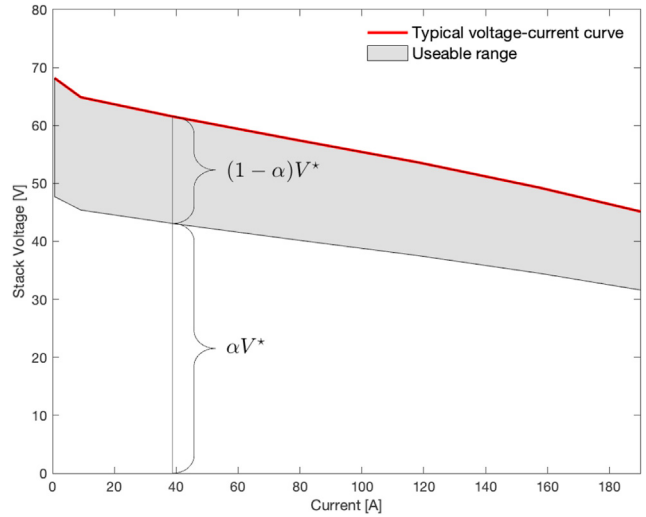
Fig. 3 − **An example depicting the useable range of a fuel cell.**

is completely specified by the mean function $m(\cdot)$ and the covariance function $k(\cdot, \cdot)$ given by

$$m(i_j) = \mathbb{E}[f(i_j)], \quad (11)$$

$$k(i_j, i_k) = \mathbb{E}[(f(i_j) - m(i_j))(f(i_k) - m(i_k))], \quad (12)$$

for all j, $k \in \{1, ..., m\}$. The covariance functions, or kernel functions, can take various forms, such as the Matern 3/2 kernel given by

$$k(i_j, j_k) = \sigma_f^2\left(1 + \frac{\sqrt{3}\,\bar{r}}{\sigma_l^2}\right)\exp\left\{-\frac{\sqrt{3}\,\bar{r}}{\sigma_l^2}\right\} \quad (13)$$

for all j, $k \in \{1, ..., m\}$, where $\bar{r} = |i_j - i_k|$ is the distance between i_j and i_k, and σ_f and σ_l are parameters of the kernel.

Describing the GP defined in (11) and (12) into vector form for V^m, cf. (1), yields

$$V^m = \begin{bmatrix} V_1 \\ \vdots \\ V_m \end{bmatrix} = \begin{bmatrix} f(i_1) + Z \\ \vdots \\ f(i_m) + Z \end{bmatrix} \sim \mathcal{N}(\boldsymbol{\mu}_V, \boldsymbol{\Sigma}_W), \quad (14)$$

where

$$\boldsymbol{\mu}_V = [m(i_1), ..., m(i_m)]^T, \quad (15)$$

$$\boldsymbol{\Sigma}_W = \mathbf{K}(i, i) + \sigma^2 I = \begin{bmatrix} k(i_1, i_1) & \cdots & k(i_1, i_m) \\ \vdots & \ddots & \vdots \\ k(i_m, i_1) & \cdots & k(i_m, i_m) \end{bmatrix} + \sigma^2 I, \quad (16)$$

and I is the identity matrix of proper dimension. Conditioning the joint Gaussian distribution on the training sample yields the prediction of $\overline{V}(\bar{i})$ given by

$$\overline{V}|V^m, \boldsymbol{v}, \bar{i} \sim \mathcal{N}\left(\mu_{\overline{V}}, \sigma_{\overline{V}}^2\right), \quad (17)$$

where

$$\mu_{\overline{V}} = \mathbf{K}(\bar{i}, i)[\mathbf{K}(i, i) + \sigma^2 I]^{-1}\boldsymbol{v}, \quad (18)$$

$$\sigma_{\overline{V}}^2 = k(\overline{i}, \overline{i}) - \mathbf{K}(\overline{i}, \mathbf{i})[\mathbf{K}(\mathbf{i}, \mathbf{i}) + \sigma^2 \mathbf{I}]^{-1} \mathbf{K}(\mathbf{i}, \overline{i}), \tag{19}$$

and $\boldsymbol{v}$ is a realization of V^m.

It is easy to see that learning a GP from the training samples boils down to the learning of the kernel parameters, e.g. $\boldsymbol{\theta} = \left[\sigma, \sigma_f, \sigma_l\right]^T$ for the Matern 3/2 kernel, which is usually obtained by maximizing the logarithm likelihood function via a gradient-based algorithm [44, Chapter 6.4.3].

Rate distortion results for performance measure

Given the distribution of the voltage in (14), the user is able to evaluate the performance of the fuel cell. However, the user has only access to samples of the distribution, rather than the distribution, when the fuel cell is operating. A perfect estimate of the performance measure requires infinitely many samples of the distribution, so the performance estimate is never perfect [42, pp.301]. To evaluate the "goodness" of the performance estimate using a finite number of samples, a distortion measure is required to evaluate the difference between the performance and the estimate. Rate distortion theory provides the minimum number of samples needed to achieves a particular distortion value.

The rate distortion theory problem is depicted in Fig. 4. The source is denoted as V^m; the performance measure that is obtained via (4) is denoted by the random variable η_m; the encoder describes the realizations of η_m by an index $g\left(\eta_m\right) \in \{1, 2, ..., 2^R\}$, and the decoder represents η_m by an estimate $\widehat{\eta}_m$. Here R is the number of bits used to represent η_m, usually called the rate. Then for a given distortion measure $d(\eta_m, \widehat{\eta}_m)$, the problem of finding the minimum bits needed to achieve an arbitrary distortion value is given by

$$R(D) = \min_{\mathbb{E}[d(\eta_m, \widehat{\eta}_m)] \leq D} R. \tag{20}$$

Shannon shows in [45] that finding the minimum number of bits is equivalent to solving the problem given by

$$R(D) = \min_{\mathbb{E}[d(\eta_m, \widehat{\eta}_m)] \leq D} I(\eta_m, \widehat{\eta}_m) \tag{21}$$

for the asymptotic scenario, where $I(\eta_m, \widehat{\eta}_m)$ is the mutual information between η_m and $\widehat{\eta}_m$. However, solving the problem in (21) is quite challenging in general, and closed-form expressions are usually unavailable, especially for η_m defined in (4).

Consider the square error distortion given by

$$d(\eta_m, \widehat{\eta}_m) = (\eta_m - \widehat{\eta}_m)^2, \tag{22}$$

which is also the mean square error (MSE) of the estimation, the following theorem provides an upper bound for a source with fixed variance and square error distortion case.
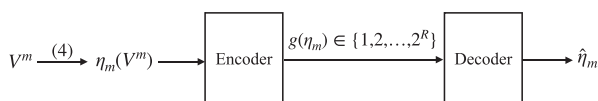
Theorem 1. [46, pp. 5] *For the square error distortion in* (22), *the rate distortion function of random variable X with variance $\widetilde{\sigma}^2$ is bounded as*

$$R(D) \leq \frac{1}{2} \log \frac{\widetilde{\sigma}^2}{D} \quad \text{when } 0 \leq D \leq \widetilde{\sigma}^2 \tag{23}$$

or

$$R(D) = 0 \quad \text{when } D > \widetilde{\sigma}^2, \tag{24}$$

in which the upper bound in (23) *is achieved when X follows a Gaussian distribution.*

This theorem states that compared with other sources, the Gaussian source requires the largest number of bits to describe it with the same distortion under quadratic cost and second order constraints. This implies that if the number of bits allows the Gaussian source to achieve a given distortion, then same number of bits achieves a smaller distortion for any other source. In the following we will use this insight to characterize the number of samples needed to describe η_m.

Thus, we use the results in Theorem 1 to propose the following upper bound.

Theorem 2. *For the functional performance measure η_m defined in* (4) *and the square error distortion $d(\eta_m, \widehat{\eta}_m) = (\eta_m - \widehat{\eta}_m)^2$, the rate distortion function is upper bounded by*

$$R(D) \leq \frac{1}{2} \log \frac{\sigma_{\eta_m}^2}{D}, \quad \text{when } 0 \leq D \leq \sigma_{\eta_m}^2 \tag{25}$$

or is equal to 0 when $D \geq \sigma_{\eta_m}^2$, where $\sigma_{\eta_m}^2$ is the variance of η_m.

Theorem 2 shows that when the number of samples of η_m satisfies

$$n \geq 2^{R(D)} = 2^{\frac{1}{2}\log \frac{\sigma_{\eta_m}^2}{D}}, \tag{26}$$

then $\mathbb{E}[(\eta_m - \widehat{\eta}_m)^2] \leq D$. Note that the number of samples needed to describe η_m is equivalent to the number of samples needed to describe V^m. Thus the number of samples needed for V^m is also n.

Although the result in Theorem 2 is for the functional performance measure, it is easy to extend the result to the generalized performance measure case. Replacing the variance of η_m with the variance of $(\eta_m)_g$ provides the rate distortion results for the generalized performance measure $(\eta_m)_g$.

The calculation of the variance for η_m is challenging even when V^m is modelled by a GP. The value of $\sigma_{\eta_m}^2$ can be estimated via Monte Carlo methods, i.e. generating realizations of η_m through samples of V^m.

Sensing strategy for voltage vector

The parameters that represent the working state of the fuel cell are usually observed at a given frequency, which generates a large amount of fuel cell data and occupies substantial storage space. For example, there are 85 types of observations obtained simultaneously for the fuel cells used by the OEM. In addition to the parameters of the fuel

$$V^m \xrightarrow{(4)} \eta_m(V^m) \longrightarrow \boxed{\text{Encoder}} \xrightarrow{g(\eta_m) \in \{1,2,...,2^R\}} \boxed{\text{Decoder}} \longrightarrow \widehat{\eta}_m$$

Fig. 4 – Graphical description of the rate distortion problem.

cell, some other parameters that describe the state of the whole vehicle are also acquired simultaneously. While uniform sampling schemes provide a robust estimation performance for processes with low correlation between samples, the multivariate Gaussian structure between voltage and current points can be exploited to derive optimal linear observation procedures [47]. Since in our setting we are limited to sampling voltage and current pairs, in the following, we propose an algorithm to identify the current points for which the corresponding voltages carry more information about the voltage vector. This solution enables the user to acquire and store a reduced amount of voltage data and to estimate voltage accurately in the unobserved current points.

The scenario in which the user only observes K state variables of the vector of voltages is mathematically characterized by

$$\widetilde{V}^K = HV^m + Z^K, \tag{27}$$

where $H \in \mathbb{R}^{K \times m}$ is given by

$$H = \left[e_{a_1}^{\mathrm{T}} \; ; \; \dots \; ; \; e_{a_K}^{\mathrm{T}} \right], \tag{28}$$

$\widetilde{V}^K \in \mathbb{R}^K$ is the vector of observed elements of V^m, e_j is a vector of proper dimension with value 1 for the j-th entry and 0 elsewhere; and $\mathcal{S} = \{a_1, \dots, a_K\}$ is the set of indices of the observed state variables. The system noise Z^K is assumed to be white noise, i.e. $Z^K \sim \mathcal{N}(\mathbf{0}, \sigma^2 I)$ with the variance of the noise is determined by the Gaussian process in (14).

Denoting the vector of unobserved elements by $V_{uo}^{m-K} \in \mathbb{R}^{m-K}$, then the joint distribution of the observed elements and the unobserved elements is

$$\begin{bmatrix} \widetilde{V}^K \\ V_{uo}^{m-K} \end{bmatrix} \sim \mathcal{N}\left(\begin{bmatrix} m(i_o) \\ m(i_{uo}) \end{bmatrix}, \begin{bmatrix} K(i_o, i_o) + \sigma^2 I & K(i_o, i_{uo}) \\ K(i_{uo}, i_o) & K(i_{uo}, i_{uo}) \end{bmatrix} \right), \tag{29}$$

as described by the Gaussian process given in (14), where $i_o = [i_{a_1}, \dots, i_{a_K}]^{\mathrm{T}} \in \mathbb{R}^K$ is the vector of observed current points and $i_{uo} \in \mathbb{R}^{m-K}$ is the vector of unobserved current points. Conditioning the joint Gaussian distribution on $\widetilde{V}^K$ yields the distribution of V_{uo}^{m-K} [48, IV.B.49], which is given by

$$V_{uo}^{m-K} | \widetilde{V}^K, i_o, i_{uo} \sim \mathcal{N}(\boldsymbol{\mu}_{uo}, \boldsymbol{\Sigma}_{uo}), \tag{30}$$

where

$$\boldsymbol{\mu}_{uo} = K(i_{uo}, i_o) \left[K(i_o, i_o) + \sigma^2 I \right]^{-1} \widetilde{V}^K, \tag{31}$$

$$\boldsymbol{\Sigma}_{uo} = K(i_{uo}, i_{uo}) - K(i_{uo}, i_o) \left(K(i_o, i_o) + \sigma^2 I \right)^{-1} K(i_o, i_{uo}). \tag{32}$$

The conditional mean of V_{uo}^{m-K}, i.e. $\boldsymbol{\mu}_{uo}$, is exactly the estimator that minimizes the MSE [48, IV.B.50] given by

$$\mathbb{E}_{\widetilde{V}^K} \left[\mathbb{E}_{V_{uo}^{m-K}} \left[\| V_{uo}^{m-K} - \widehat{V}_{uo}^{m-K}(\widetilde{V}^K) \|_2^2 | \widetilde{V}^K \right] \right], \tag{33}$$

where $\widehat{V}_{uo}^{m-K}$ is the estimate of V_{uo}^{m-K}, and the resulting MSE is given by

$$\mathbb{E}_{\widetilde{V}^K} \left[\mathbb{E}_{V_{uo}^{m-K}} \left[\| V_{uo}^{m-K} - \boldsymbol{\mu}_{uo} \|_2^2 | \widetilde{V}^K \right] \right] = \mathrm{tr}(\boldsymbol{\Sigma}_{uo}). \tag{34}$$

Now the problem boils down to finding the K state variables that convey the maximum information about the state of the fuel cell. We adopt an information-theoretic framework to solve this problem, and choose the state variables that hold more information about voltage. The state variables selection procedure is cast as the following optimization problem.

$$\max_{H} \quad I(\widetilde{V}^K; V^m) \tag{35}$$

$$\text{s.t.} \quad |\mathcal{S}| = K, \tag{36}$$

where $|\mathcal{S}|$ denotes the cardinality of set $\mathcal{S}$, i.e. the number of elements in $\mathcal{S}$. The optimization problem in (35) and (36) is challenging due to the combinatorial character of the selection problem, i.e. there is no efficient algorithm to find the optimal solution. In the following, we propose a greedy algorithm to address this challenge.

The mutual information objective in (35) is reformulated using the chain rule of mutual information [42, Theorem 2.5.2] to yield

$$I(\widetilde{V}^K; V^m) = I(\widetilde{V}_1, \dots, \widetilde{V}_K; V^m) \tag{37}$$

$$= \sum_{i=1}^{K} I(\widetilde{V}_i; V^m | \widetilde{V}_{i-1}, \widetilde{V}_{i-2}, \dots, \widetilde{V}_1). \tag{38}$$

The proposed greedy algorithm aims to maximize the conditional mutual information at each iteration to maximize the mutual information $I(\widetilde{V}^K; V^m)$. Assume that the user observes K elements of vector V^m and proceeds to select the $(K+1)$-th element from the unobserved elements to observe. By observing the $(K+1)$-th element, the mutual information gain is obtained by the chain rule as

$$I(\widetilde{V}_{K+1}; V^m | \widetilde{V}_K, \widetilde{V}_{K-1}, \dots, \widetilde{V}_1) = I(e_{\tilde{a}}^{\mathrm{T}} V_{uo}^{m-K}; V_{uo}^{m-K}), \tag{39}$$

where $\tilde{a} \in \{1, \dots, m-K\}$.

Given the fact that V_{uo}^{m-K} is a Gaussian random variable and $e_{\tilde{a}}$ is a linear vector in (27), it holds that

$$e_{\tilde{a}}^{\mathrm{T}} V_{uo}^{m-K} \sim \mathcal{N}(e_{\tilde{a}}^{\mathrm{T}} \boldsymbol{\mu}_{uo}, e_{\tilde{a}}^{\mathrm{T}} \boldsymbol{\Sigma}_{uo} e_{\tilde{a}} + \sigma^2). \tag{40}$$

The mutual information between the candidate variable and the unobserved variables is given by [49, Proposition 2]

$$I(e_{\tilde{a}}^{\mathrm{T}} V_{uo}^{m-K}; V_{uo}^{m-K}) = \frac{1}{2} \log \frac{|\boldsymbol{\Sigma}_{uo}| |e_{\tilde{a}}^{\mathrm{T}} \boldsymbol{\Sigma}_{uo} e_{\tilde{a}} + \sigma^2|}{|\boldsymbol{\Sigma}|}, \tag{41}$$

where $\boldsymbol{\Sigma}$ is the covariance matrix of the joint distribution of $(V_{uo}^{m-K}, \widetilde{V}_{K+1})$, and is given by

$$\boldsymbol{\Sigma} = \begin{bmatrix} \boldsymbol{\Sigma}_{uo} & \boldsymbol{\Sigma}_{uo} e_{\tilde{a}} \\ e_{\tilde{a}}^{\mathrm{T}} \boldsymbol{\Sigma}_{uo} & e_{\tilde{a}}^{\mathrm{T}} \boldsymbol{\Sigma}_{uo} e_{\tilde{a}} + \sigma^2 \end{bmatrix}. \tag{42}$$

Thus, maximizing the mutual information given in the right-hand side of (39) is equivalent to solving

$$\max_{\tilde{a}} \log |e_{\tilde{a}}^{\mathrm{T}} \boldsymbol{\Sigma}_{uo} e_{\tilde{a}} + \sigma^2|. \tag{43}$$

The solution to (43) is obtained by choosing the diagonal entry of $\boldsymbol{\Sigma}_{uo}$ with the largest value. Based on the analysis given

above, we propose the greedy algorithm in Algorithm 1, in which $\mathbb{1}_{\{\cdot\}}$ is the indicator function.

Algorithm 1 Selection of K state variables that maximize mutual information

---

Input: number of state variables K, kernel matrix $\mathbf{K}(\cdot,\cdot)$, the current vector $\mathbf{i}$, variance of system noise σ^2
Output: $\mathcal{S}$
1: Initialization: $\mathcal{S} = \emptyset$, $k = 1$, $\boldsymbol{\Sigma}_{uo} = \boldsymbol{\Sigma}_{VV}$
2: **while** $k \le K$ **do**
3:　　Set $\tilde{a} = \underset{\tilde{a}}{\operatorname{argmax}}\ (\boldsymbol{\Sigma}_{uo})_{\tilde{a}\tilde{a}}$
4:　　Set $a_k = \sum_{j=1}^{m} j \mathbb{1}_{\{(\mathbf{i}_{uo})_{\tilde{a}} = \mathbf{i}_j\}}$
5:　　Set $\mathcal{S} = \mathcal{S} \bigcup a_k$, $k = k+1$
6:　　Update V_{uo} according to $\mathcal{S}$, update $\boldsymbol{\Sigma}_{uo}$ according to (32)
7: **end while**

Case study

While the results in the paper are general and apply to fuel cells or other power sources in general, we validate the proposed analytical framework by studying the performance of real fuel cells with data provided by the OEM. The case study enables us to discuss the insight provided by the numerical results obtained with the proposed framework and to demonstrate the applicability of our approach. The rated electrical power of the fuel cell adopted by the OEM is 8.5 kW, the operating current is between 0 A and 200 A, and the operating voltage is between 40 V and 80 V. The typical V−I curve is given in Fig. 1b, which provides the user with a guideline for determining the performance of the fuel cell.

The dataset from the OEM is been acquired during experiments carried out 118 times, from which 3,000,907 data points, i.e. $\{v, i\}_{j=1}^{3,000,907}$, are obtained. The data points are shown in Fig. 5a, in which the typical V−I curve is also plotted as comparison. Our main focus is to model the voltage distribution via the GP and to obtain the minimum number of samples that are needed to describe the source to achieve a given distortion. So we use the majority of the dataset to train the GP and the rest to assess the validity of the obtained GP. To that end, we separate the complete dataset into two sets, i.e. the training set and the validation set, which include 297,898 and 3,009 data points.

Performance measure for fuel cell

Fig. 5b shows the pointwise performance measure η defined in (3) and the worst-case performance $\underline{\eta}$ that is defined in (7) for the dataset when $L = 1$. Note that changing the value of L only scales the performance measure, so without loss of generality, we only show the case that $L = 1$. It can be seen that the fuel cell has good average performance for different currents, except for the performance degradation at 144 A. This indicates the need to check the condition of the fuel cell around 144 A. For the worst-case performance, although the performance is satisfactory, the performance for medium values of current is worse than the performance for low and high values of current. Fig. 5c shows the histogram of the average performance defined in (6) when $L = 1$. It can be seen

that the fuel cell displaces good overall performance except for one case. In summary, the fuel cell exhibits good performance overall on the proposed measures, which coincides with the assessment of the manufacturer during the regular check.

The conclusion drawn using the pointwise performance measure is the same as the one using the generalized performance measure. So in the following we only show the results for the pointwise performance measure.

Voltage vector modeling via a Gaussian process

As mentioned in the preceding text, the kernel functions for GP are of various structures to reflect the correlation structure of the voltages at different current points. After comparing the performance of several kernel functions on the training set, we choose the Matern 3/2 kernel given in (13) in the following, which is the one that induces the least regression loss.

Fig. 6a shows the performance of the Matern 3/2 kernel on the training set. As any finite number of a GP have a joint Gaussian distribution, the marginal distribution of V^m, i.e. the distribution of each V_i, $i \in [1, ..., m]$, is also a univariate Gaussian distribution. The 99.7% confidence interval, i.e. three-sigma interval, of the constructed GP is depicted in Fig. 6a by the shadowed area. As mentioned in (14), the confidence interval of the GP on the training set incorporates the uncertainty introduced by the system noise. It can be observed that the constructed GP has a good performance on the training set.

As mentioned in the preceding text, our main goal is to use the structure of the GP to analyze the rate-distortion function, rather than simply predicting the voltage. We only show the prediction results on 400 data points in Fig. 6b, which forms a complete running sequence from the validation set. Note that the confidence interval of the prediction does not take the variance induced by the system noise into account. It can be seen that the constructed GP has good performance on the validation set, except in a few points whose voltage deviates from the typical value induced by the typical V−I curve.

Rate distortion results

As stated in Theorem 2, the rate distortion function under square error distortion is upper bounded by the Gaussian source with the same variance. To obtain the variance of η_m, we use a Monte Carlo approach to generate 1,258,000 samples of V^m, which is 1,000 times more samples than the dimension m.

Fig. 7a shows the rate distortion upper bound in Theorem 2 for the function performance measure η_m defined in (4) when $L = 1$. It can be seen that the variance of the performance measure is small when $L = 1$. This implies that the user needs only one sample to achieve a satisfactory estimate for η_m, which is much less than the number of bits required for practical setting. This problem can be reformulated by choosing a larger value for L, such as $L = 100,000$. Fig. 7b also shows the rate distortion upper bound in

(a)

(b)

(c)
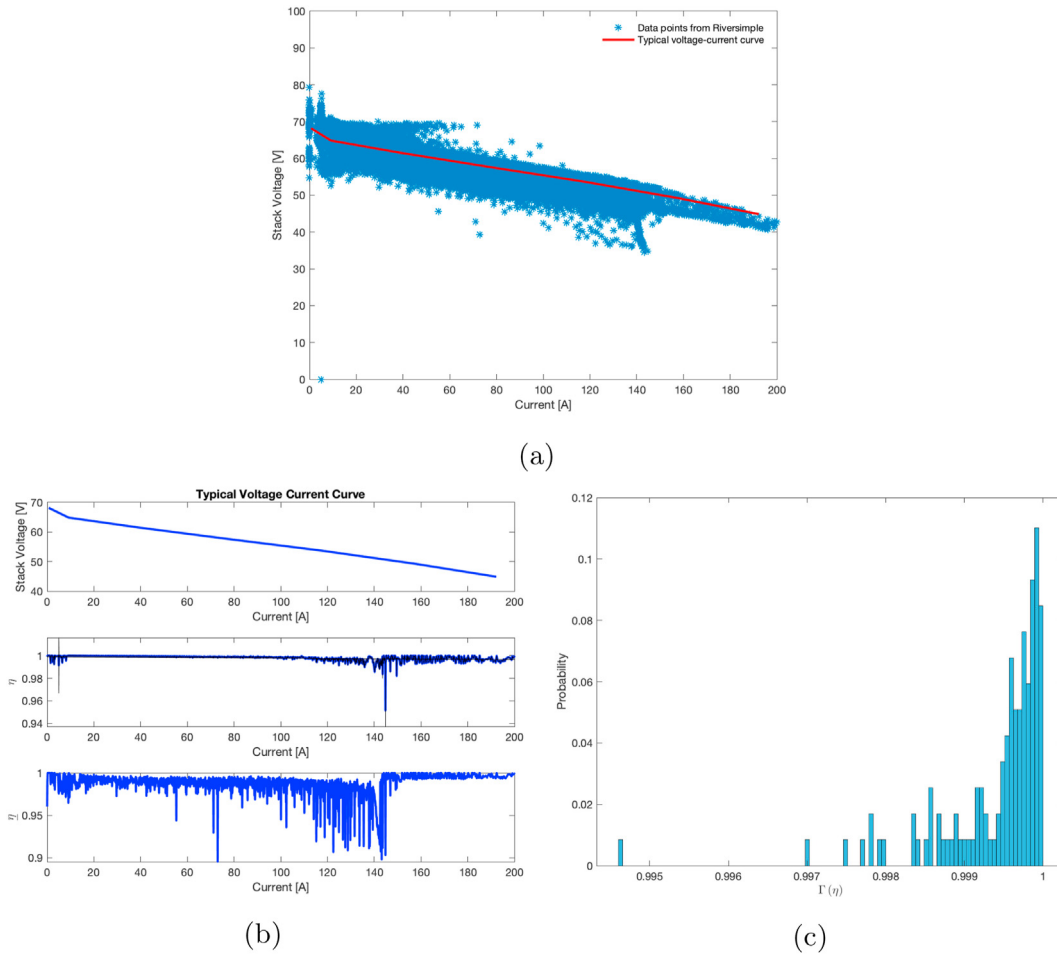
Fig. 5 − Performance analysis for the fuel cell dataset: (a) the fuel cell operating data used for the case study, (b) the pointwise performance measure η and the worst-case performance $\underline{\eta}$ for the case study when $L = 1$, (c) histogram of the average performance $\Gamma(\eta)$ for the case study when $L = 1$.

(a)

(b)
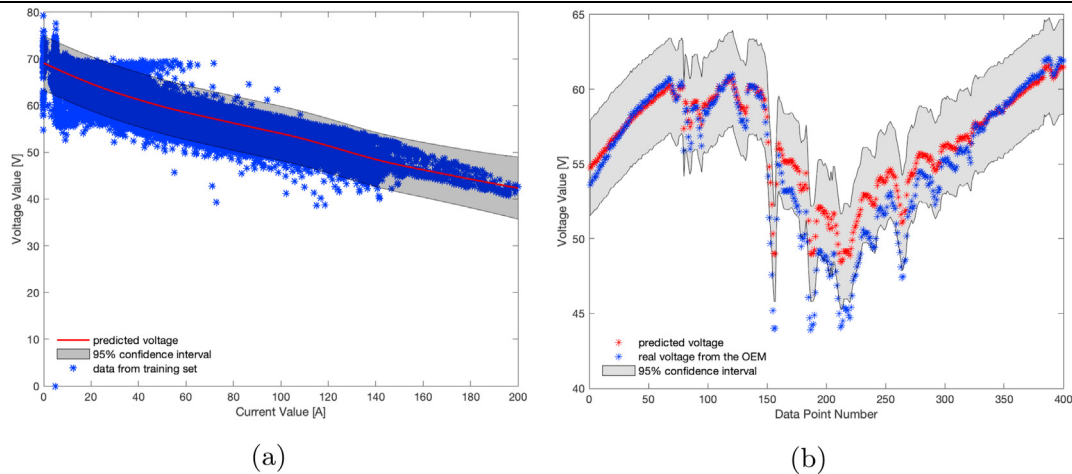
Fig. 6 − The performance of the constructed GP: (a) on the training data set, (b) on a sequence of 400 data points from the validation set.

Theorem 2 for the function performance measure η_m defined in (4) when $L = 100{,}000$, in which η_m induces larger variance. *This suggests that the user needs to choose the value of L carefully* *when characterizing the rate distortion results*. It is worth mentioning that the value of L has no effect on the performance measure.
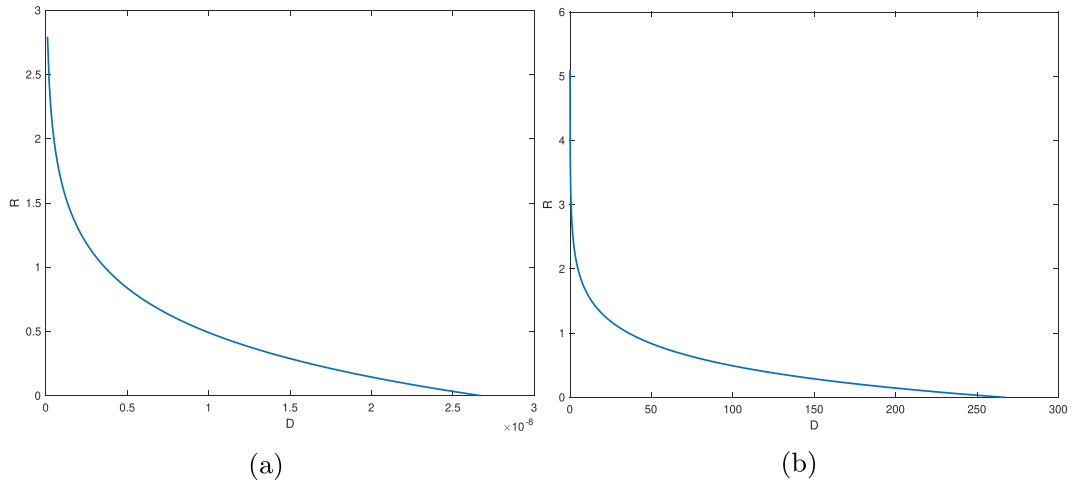
Fig. 7 – **Rate distortion upper bound for the function performance measure η_m: (a) when $L = 1$, (b) when $L = 100,000$.**

Sensing strategy

Fig. 8a shows the performance of Algorithm 1 on the mutual information objective in (35) and on the scaled MSE (SMSE) that is obtained from (34) as

$$\text{SMSE} = \frac{1}{m-K}\text{MSE} = \frac{1}{m-K}\text{tr}(\boldsymbol{\Sigma}_{uo}). \tag{44}$$

We scale the MSE by the number of entries in the vector of unobserved elements, which yields the average MSE induced
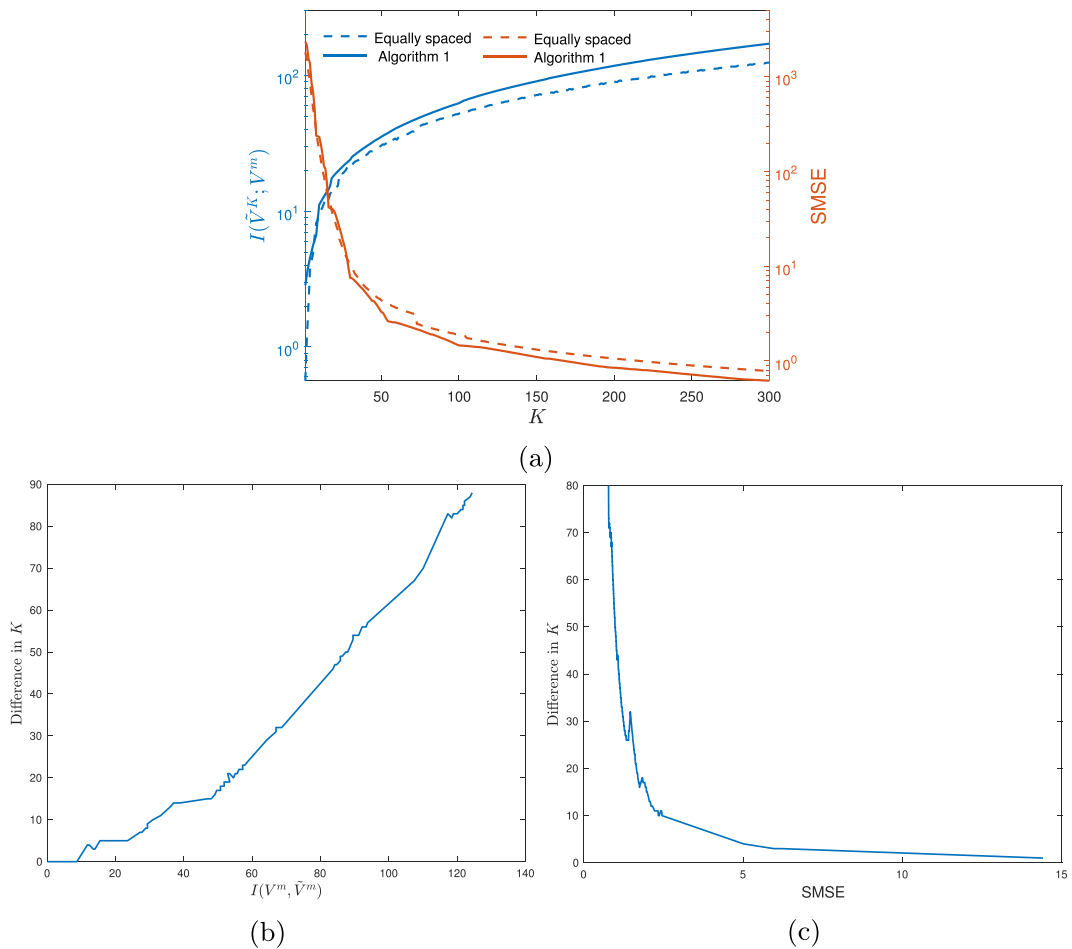

Fig. 8 – **Performance of Algorithm 1: (a) on the mutual information objective and the SMSE, (b) on the difference in K that generates the same amount of mutual information when compare with Equally space algorithm, (c) on the difference in K that generates the same value of SMSE when compare with Equally space algorithm.**

on each unobservable element. We also compare the performance of Algorithm 1 with equally spaced sampling, i.e. when the sampling points are equally distributed along the current range given by [0 A, 200 A]. It can be seen that the sampling points chosen by the proposed algorithm contain more information than the equally spaced sampling case and that the resulting SMSE of Algorithm 1 is smaller than that of the equally spaced one. It is worth mentioning that although the mutual information increases linearly with the number of observed elements, the SMSE decreases exponentially when the number of observed elements increases. Also the performance gain of Algorithm 1 in SMSE terms is more significant for large value of K.

Fig. 8b shows the difference between the value of K that Algorithm 1 requires and equally spaced sampling requires to acquire the same amount of information. Similarly, Fig. 8c shows the results for SMSE. Note that the mutual information or SMSE generated by Algorithm 1 and the equally spaced algorithm are regarded as equal when the difference between mutual information or SMSE is smaller than 0.01. When the mutual information is high, or the SMSE is low, Algorithm 1 uses fewer state variables to obtain the same amount of mutual information or the same SMSE. The advantage of Algorithm 1 increases as mutual information increases, or as SMSE decreases.

Conclusion

In this paper, we proposed a mathematical framework and the corresponding measures for the fuel cell performance evaluation from the user side. The minimum number of samples needed to characterize the performance measure is introduced via rate-distortion theory results. Furthermore, we propose a sensing strategy to identify the current points that yield high mutual information between the chosen point and the voltages. The case study with fuel cell data from the OEM shows that the performance measure fits with the observations from the manufacturer. The proposed sensing algorithm achieves high mutual information and low SMSE simultaneously for the case study.

We envision future research addressing two main challenges. Firstly, the robustness of the proposed approach to datasets generated in different operation environments, e.g. end of life performance data, needs further validation, which hinges on access to different case study data. More importantly, the generalization of the proposed technique to non-Gaussian distributions is a non-trivial problem that will have to be tackled as performance and health models are refined. The generalization to non-Gaussian distributions will provide some insight into the fundamental monitoring requirements for fuel cells that operate under a wide range of conditions.

Credit authorship contribution statement

Ke Sun: Conceptualization; Methodology; Software; Formal analysis; Writing - Original Draft. Iñaki Esnaola: Conceptualization; Methodology; Writing - Review & Editing; Supervision; Funding acquisition. Okechukwu Okorie: Resources. Fiona Charnley: Resources; Funding acquisition. Mariale Moreno: Resources. Ashutosh Tiwari: Funding acquisition.

Declaration of competing interest

The authors declare that they have no known competing financial interests or personal relationships that could have appeared to influence the work reported in this paper.

Acknowledgments

REFERENCES

[1] Committee on Climate Change. Hydrogen in a low-carbon economy. https://www.theccc.org.uk/wp-content/uploads/2018/11/Hydrogen-in-a-low-carbon-economy.pdf; 2018.

[2] Muradov NZ, Veziroğlu TN. "green" path from fossil-based to hydrogen economy: an overview of carbon-neutral technologies. Int J Hydrogen Energy 2008;33(23):6804—39.

[3] Dincer I. Technical, environmental and exergetic aspects of hydrogen energy systems. Int J Hydrogen Energy 2002;27(3):265—85.

[4] HyWeb. Hydrogen data. http://www.h2data.de/.

[5] Wang J. System integration, durability and reliability of fuel cells: challenges and solutions. Appl Energy 2017;189:460—79.

[6] Haji S. Analytical modeling of pem fuel cell i—v curve. Renew Energy 2011;36(2):451—8.

[7] Hwang JJ, Chang WR, Weng FB, Su A, Chen CK. Development of a small vehicular pem fuel cell system. Int J Hydrogen Energy 2008;33(14):3801—7.

[8] Rasha L, Cho JIS, Millichamp J, Neville TP, Shearing PR, Brett DJL. Effect of reactant gas flow orientation on the current and temperature distribution in self-heating polymer electrolyte fuel cells. Int J Hydrogen Energy 2021;46(10):7502—14.

[9] Deng B, Ye D, Zhang B, Zhu X, Chen R, Liao Q. Current density distribution in air-breathing microfluidic fuel cells with an array of graphite rod anodes. Int J Hydrogen Energy 2021;46(3):2960—8.

[10] Benmouiza K, Cheknane A. Analysis of proton exchange membrane fuel cells voltage drops for different operating parameters. Int J Hydrogen Energy 2018;43(6):3512—9.

[11] Danilov VA, Tade MO. A new technique of estimating anodic and cathodic charge transfer coefficients from sofc polarization curves. Int J Hydrogen Energy 2009;34(16):6876—81.

[12] Zhang S, Guo X, Zhang X. Multi-objective decision analysis for data-driven based estimation of battery states: a case study of remaining useful life estimation. Int J Hydrogen Energy 2020;45(27):14156—73.

[13] Zhu G, Chen W, Lu S, Chen X. Parameter study of high-temperature proton exchange membrane fuel cell using data-driven models. Int J Hydrogen Energy 2019;44(54):28958—67.

[14] Zhang C, Li W, Hu M, Cheng X, He K, Mao L. A comparative study of using polarization curve models in proton exchange membrane fuel cell degradation analysis. Energies 2020;13(15):3759.

[15] Cheng Y, Zerhouni N, Lu C. A hybrid remaining useful life prognostic method for proton exchange membrane fuel cell. Int J Hydrogen Energy 2018;43(27):12314—27.

[16] Ma R, Yang T, Breaz E, Li Z, Briois P, Gao F. Data-driven proton exchange membrane fuel cell degradation predication through deep learning method. Appl Energy 2018;231:102—15.

[17] Ardabili SF, Najafi B, Shamshirband S, Behrouz BM, Deo RC, Chau K. Computational intelligence approach for modeling hydrogen production: a review. Eng Appl Comput Fluid Mech 2018;12(1):438—58.

[18] Pukrushpan J, Stefanopoulou A, Varigonda S, Eborn J, Haugstetter C. Control-oriented model of fuel processor for hydrogen generation in fuel cell applications. Contr Eng Pract 2006;14(3):277—93.

[19] Broom DP, Webb CJ, Fanourgakis GS, Froudakis GE, Trikalitis PN, Hirscher M. Concepts for improving hydrogen storage in nanoporous materials. Int J Hydrogen Energy 2019;44(15):7768—79.

[20] Anderson G, Schweitzer B, Anderson R, Gómez-Gualdrón DA. Attainable volumetric targets for adsorption-based hydrogen storage in porous crystals: molecular simulation and machine learning. J Phys Chem C 2018;123(1):120—30.

[21] Rahnama A, Zepon G, Sridhar S. Machine learning based prediction of metal hydrides for hydrogen storage, part I: prediction of hydrogen weight percent. Int J Hydrogen Energy 2019;44(14):7337—44.

[22] Rahnama A, Zepon G, Sridhar S. Machine learning based prediction of metal hydrides for hydrogen storage, part II: prediction of material class. Int J Hydrogen Energy 2019;44(14):7345—53.

[23] Bucior BJ, Bobbitt NS, Islamoglu T, Goswami S, Gopalan A, Yildirim OK, Farha T, Bagheri N, Snurr RQ. Energy-based descriptors to rapidly predict hydrogen storage in metal—organic frameworks. Mol Syst Des Eng 2019;4(1):162—74.

[24] El-Sharkh MY, Tanrioven M, Rahman A, Alam MS. Economics of hydrogen production and utilization strategies for the optimal operation of a grid-parallel pem fuel cell power plant. Int J Hydrogen Energy 2010;35(16):8804—14.

[25] Nakano S, Washizu A. A panoramic analysis of hydrogen utilization systems: using an input-output table for next generation energy systems. Procedia CIRP 2017;61:779—84.

[26] Wang H, Morando S, Gaillard A, Hissel D. Sensor development and optimization for a proton exchange membrane fuel cell system in automotive applications. J Power Sources 2021;487:229415.

[27] Sun L, Shen J, Hua Q, Lee KY. Data-driven oxygen excess ratio control for proton exchange membrane fuel cell. Appl Energy 2018;231:866—75.

[28] Li HW, Xu BS, Du CH, Yang Y. Performance prediction and power density maximization of a proton exchange membrane fuel cell based on deep belief network. J Power Sources 2020;461:228154.

[29] Xu D, Jiang B, Liu F. Improved data driven model free adaptive constrained control for a solid oxide fuel cell. IET Control Theory & Appl 2016;10(12):1412—9.

[30] Wu X, Xu YW, Zhao DQ, Li ZH, Zhong XB, et al. Fault detection and assessment for solid oxide fuel cell system gas supply unit based on novel principal component analysis. J Power Sources 2019;436:226864.

[31] Li Z, Outbib R, Giurgea S, Hissel D, Li Y. Fault detection and isolation for polymer electrolyte membrane fuel cell systems by analyzing cell voltage generated space. Appl Energy 2015;148:260—72.

[32] Li Z, Outbib R, Giurgea S, Hissel D, Giraud A, Couderc P. Fault diagnosis for fuel cell systems: a data-driven approach using high-precise voltage sensors. Renew Energy 2019;135:1435—44.

[33] Napoli G, Ferraro M, Sergi F, Brunaccini G, Antonucci V. Data driven models for a pem fuel cell stack performance prediction. Int J Hydrogen Energy 2013;38(26):11628—38.

[34] Li Z, Outbib R, Hissel D, Giurgea S. Data-driven diagnosis of pem fuel cell: a comparative study. Contr Eng Pract 2014;28:1—12.

[35] Mao L, Jackson L. Selection of optimal sensors for predicting performance of polymer electrolyte membrane fuel cell. J Power Sources 2016;328:151—60.

[36] Ma R, Breaz E, Liu C, Bai H, Briois P, Gao F. Data-driven prognostics for pem fuel cell degradation by long short-term memory network. In: Proc. IEEE transportation electrification conf. and expo; 2018. p. 102—7. Long Beach, CA, USA.

[37] Barzegari MM, Rahgoshay SM, Mohammadpour L, Toghraie D. Performance prediction and analysis of a dead-end pemfc stack using data-driven dynamic model. Energy 2019;188:116049.

[38] Wang B, Xie B, Xuan J, Jiao K. Ai-based optimization of pem fuel cell catalyst layers for maximum power density via data-driven surrogate modeling. Energy Convers Manag 2020;205:112460.

[39] Chavan SL, Talange DB. Modeling and performance evaluation of pem fuel cell by controlling its input parameters. Energy 2017;138:437—45.

[40] Heidary H, Kermani MJ, Dabir B. Influences of bipolar plate channel blockages on pem fuel cell performances. Energy Convers Manag 2016;124:51—60.

[41] Wang L, Husar A, Zhou T, Liu H. A parametric study of pem fuel cell performances. Int J Hydrogen Energy 2003;28(11):1263—72.

[42] Cover TM, Thomas JA. Elements of information theory. John Wiley & Sons; 2012.

[43] Rasmussen CE, Williams CKI. Gaussian processes for machine learning. Cambridge, MA, USA: MIT press; 2006.

[44] Bishop C. Pattern recognition and machine learning. New York: Springer-Verlag; 2006.

[45] Shannon CE. Coding theorems for a discrete source with a fidelity criterion. IRE Nat Conv Rec 1959;4(1):142—63.

[46] Gibson J. Rate distortion functions and rate distortion function lower bounds for real-world sources. Entropy 2017;19(11):604—25.

[47] Esnaola I, Tulino AM, Garcia-Frias J. Linear analog coding of correlated multivariate Gaussian sources. IEEE Trans Commun 2013;61(8):3438—47.

[48] Poor HV. An introduction to signal detection and estimation. New York: Springer; 1994.

[49] Sun K, Esnaola I, Perlaza SM, Poor HV. Stealth attacks on the smart grid. IEEE Trans Smart Grid 2020;11(2):1276—85.